Monte Carlo Simulations Studies in Small Animal PET using GATE

S. Branco[1], S. Jan[2] and P. Almeida[1]

[1]Universidade de Lisboa, Faculdade de Ciências, Instituto de Biofísica e Engenharia Biomédica, Lisboa, Portugal
[2]CEA/DSV/I[2]BM, Service Hospitalier Frédéric Joliot, Orsay, France

***Abstract*–This work is focused on the use of a simulation system dedicated for small animal PET imaging, in order to produce realistic simulated mouse exams. Sets of gold standard images where physical effects not taken into account are presented. A preliminary approach of the physiological process of the respiratory motion and the implementation of a lung tumor is shown in this paper. The quantitative and qualitative simulated data results show a good agreement with the real values.**

I. INTRODUCTION

Monte Carlo simulations are an important tool in the study of medical imaging modalities such as PET and SPECT: in designing new medical imaging devices, optimising data acquisition protocols, developing and assessing tomographic image reconstruction algorithms or evaluating correction methods for improved image quantification. We have used the Geant4 Application for Tomographic Emission (GATE) Monte Carlo platform [1] for modelling the microPET® FOCUS 220 system and for implementing realistic phantoms for small animal imaging. The aim of this work was to produce realistic simulated exams for the [^{18}F]fluoride and the 2-Deoxy-[^{18}F]fluoro-D-glucose (FDG) radiotracers using the validated microPET® FOCUS 220 system for the GATE platform and real mouse phantoms descriptions, under realistic conditions. These simulations provide a high quality set of mouse PET simulated data useful to the improvement of imaging protocols and image quantification.

II. MATERIAL AND METHODS

A. *The GATE platform*

GATE is a generic Monte Carlo simulation platform dedicated to nuclear medicine, based on Geant4 libraries, a well-established code for the simulation of radiation transport. GATE encapsulates the Geant4 libraries to achieve a modular, versatile and scripted simulation toolkit adapted to emission and transmission tomography. The use of GATE facilitates the description of different components necessary for the accurate modelling of a PET or a SPECT system, starting from the geometry up to the creation of a processing chain for the detected events. It allows describing time-dependent phenomena such as detector or patient movements, source decay kinetics and dead time for coincidence acquisitions including delay coincidences measurement.

B. *The microPET® FOCUS 220 modelling*

We modelled the microPET® FOCUS 220 system within the GATE platform. This system is suitable for acquire high resolution images of small animal as rodents and small primates [2]. The complete validation results of the microPET® FOCUS 220 simulation system using GATE can be found in [3].

C. *Mouse phantoms descriptions*

The MOBY phantom combines the realism of a voxelized phantom, with the flexibility of a mathematical phantom, based on non-uniform rational B-splines (NURBS) [4]. The phantom also includes 4D models of the mouse's cardiac and respiratory motions. We applied a resampling on the default matrix to reduce the voxel number to 40×40×124 voxels with a voxel unit size of 0.5×0.5×0.5 mm^3, this method allowed us to significantly reduce the computational time resulting from the particle tracking inside the simulated volume. The MOBY respiratory motion was set up to be dependent on two time varying parameters: change in the height of the diaphragm (Δ_{diaphr}) and the amount of chest expansion (Δ_{AP}). In the default MOBY configuration, normal breathing, the $\Delta_{diaphr.}$ was set to be 1.0 mm while the Δ_{AP} is 0.7 mm. We manipulated these parameters to produce physiological "stress breathing": the $\Delta_{diaphr.}$ was set to 4.2 mm and the Δ_{AP} was set to 6.0 mm. A set of 10 temporal frames of 0.037 s was generated over a complete respiratory cycle, illustrated by the Fig. 1. We used this phantom to implement a lung lesion and model the tumor motion as a function of the mouse breathing, as it's shown in the Fig. 2. The calculation of the motion was based on the movement of the centre of the lesion, for the non normal tidal breathing condition.

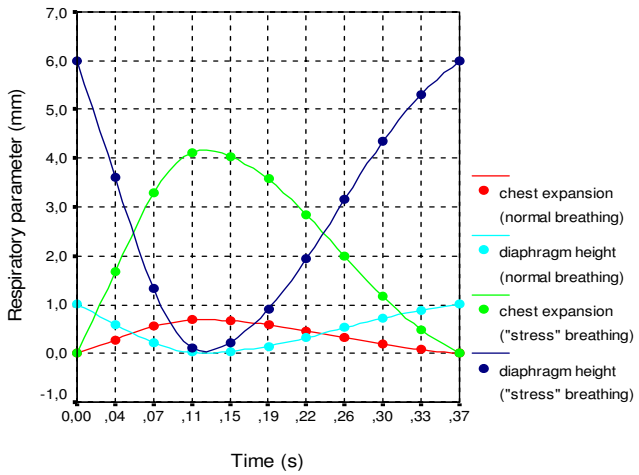

Fig. 1. Parameter curves for "normal" and "stress" breathing within MOBY.

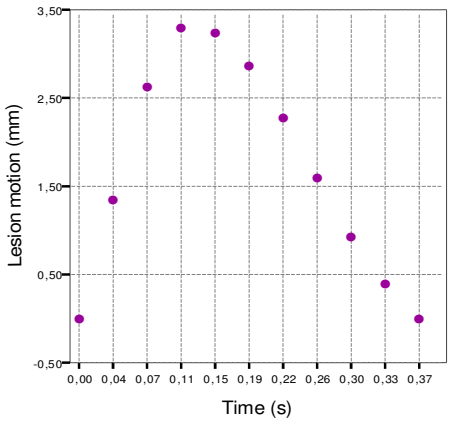

Fig. 2. Parameter curve for a lung lesion, under a "stress" breathing condition, in the MOBY phantom.

The generation of realistic mouse phantoms using real data allowed us to obtain 4D maps of the source distributions, for the case of the two different radiotracers used: [^{18}F]fluoride and FDG. Data acquisition were done at CEA/SHFJ using the microPET® FOCUS 220. An usual exam for bone imaging, in a small animal, consisted of an injection of 400 µCi of [^{18}F]fluoride and a 60 minutes acquisition time (20 minutes post injection). Data was binning with 4 frames of 900 s each. To perform a dynamic whole body mouse FDG exam, a mouse was injected with an activity of 220 µCi and scanned during 90 minutes. Data was binned with 18 frames, organized in: 5 frames of 60 s, 5 frames of 120 s, 3 frames of 300 s, 3 frames of 600 s and 2 frames of 900 s.

D. Simulation set-up

The activity distribution was set according to the activity distribution assigned to the different whole body structures for the [^{18}F]fluoride and the FDG radiotracers, respectively. The FDG biodistribution was defined by the Time Activity Curves (TACs). Fig. 3 shows the TACs for each organ obtained for the FDG mouse exam, as previously described. Regions of Interest (ROIs) were drawn around the bladder, heart, liver, kidneys and whole body. The activity in each organ was normalized to the total body activity to obtain a relative concentration for each organ at each time point.

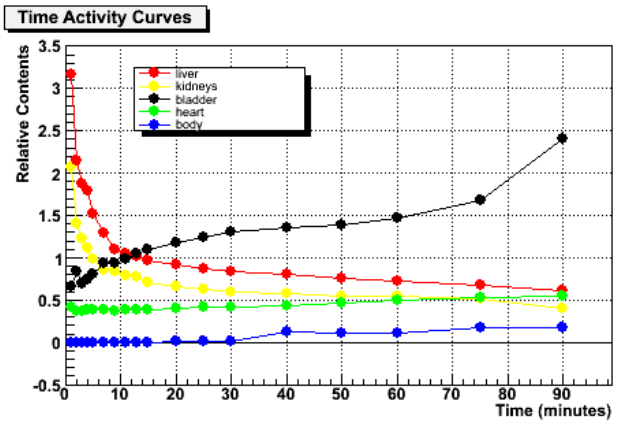

Fig. 3. Measured TACs used as input in FDG uptake simulation.

In all simulations performed, physical effects like the positron range, gamma accolinearity, tissue attenuation and scattering inside the mouse bodies were not taken into account in order to obtain gold standard data, to define the optimal results that one could obtain with a dedicated scanner and a specific radiotracer, and to speed up the computing time. Simulated results were reconstructed with FORE+OSEM2D (16 subsets and 4 iterations) algorithms, using the commercial protocols available on the scanner. Real data was reconstructed using the same method.

E. Simulation of bone imaging using [^{18}F]fluoride

With the MOBY phantom we produced a simulation of 4.0×10^{10} particles, which is equivalent to 2.21 mCi of injected dose and an acquisition time of 500 s for the last time frame. The simulation was computed on a cluster of 50 CPUs and took approximately 21h30'. This simulation corresponds to an exam where 0.5 mCi are imaged by the microPET FOCUS® 220 during 30 minutes.

The last acquisition time frame was simulated for the phantom generated from the real acquisition. In the simulation 9.6×10^{9} particles were collected, which corresponds to 284 µCi for the whole body during a 900 s acquisition time. The simulation ran on a cluster of 50 CPUs with a global computing time of 10h36'.

F. Simulation of metabolic imaging using FDG

For the last acquisition time frame we simulated, in the MOBY phantom, 131 µCi for a 15 minutes acquisition time. 4.2×10^{9} particles were tracked during 14h32' on a cluster of 10 CPUs. With the mouse phantom, generated from the real exam, the defined activity map distribution was set up to be representative of real data by assigning minimum and maximum values of measured within a specific body region to intervals of voxel values. A full simulation of 3.5×10^{9} particles was performed. We set an activity of 112 µCi for a 15 minutes acquisition time (corresponding to the last time frame). The simulation ran on a cluster of 10 CPUs with a global computing time of 12h31'.

With MOBY we reproduced a complete FDG exam were 3.4×10^{10} particles were tracked for an acquisition time of 90 minutes, corresponding to an injected dose of 220 µCi.

We used the manipulated feature of the MOBY phantom to simulate a first preliminary approach for the non normal tidal breathing (as previously described). The simulation ran on a cluster of 10 CPUs during 24h, corresponding to an acquisition time of 568.5 s for the last frame. 3.5×10^{8} particles were generated per each phantom frame (time point in the breathing cycle), corresponding to a total of approximately 3.5×10^{9}.

We implemented a lung lesion on the MOBY phantom to reproduce the last frame of an FDG exam. 4.4×10^{9} particles were generated in the mouse body corresponding to an injected dose of 131 µCi for 900 s acquisition time.

Following these last two acquisition protocols, a simulation including the motion of the lung lesion was performed with the MOBY phantom for the stress breathing. The dynamic 3D emission assumed an event collection during 900 s, where 5.6×10^{9} particles were generated.

III. RESULTS

A. *Bone imaging using ^{18}[F]fluoride*

Bone imaging simulation results are presented in Fig. 4.

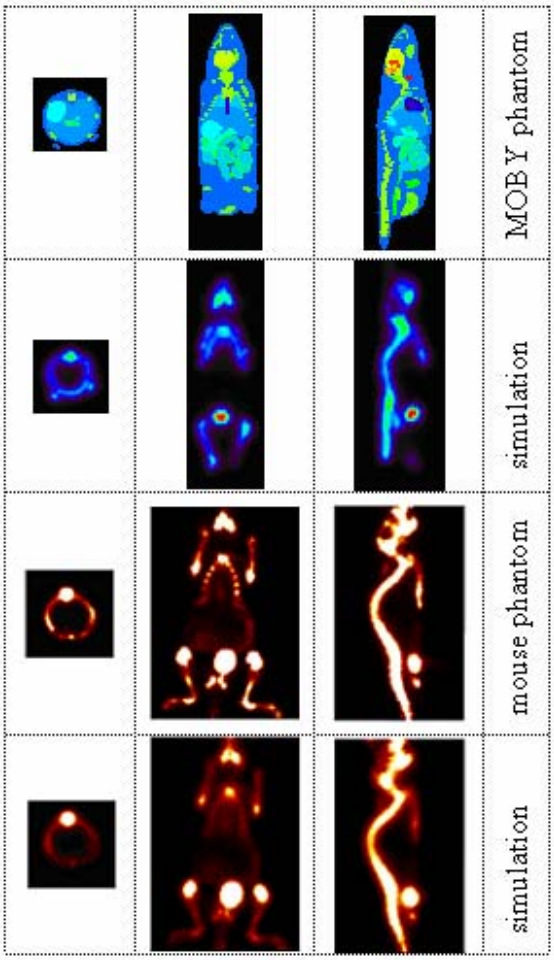

Fig. 4. Gold standard simulation for the [^{18}F]fluoride radiotracer for both the MOBY and the mouse phantom.

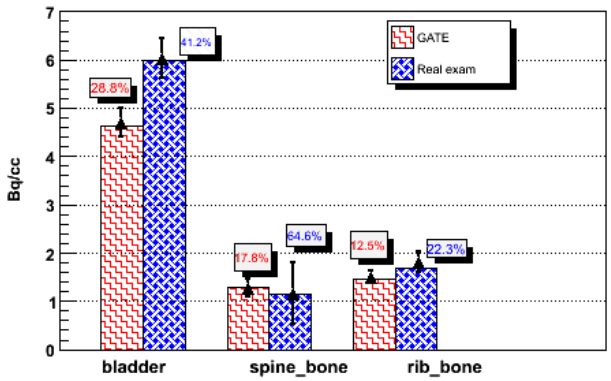

Fig. 5. Comparison between PET image quantification and the GATE measurements. Black bars represent the ROI statistical error measured as the ratio standard deviation over mean for all pixels considered.

To validate the accuracy of the simulations quantitative output we compared the real data against the simulated data, for the simulation with the phantom generated from the real exam, as illustrated in Fig. 5. We defined ROIs on the bladder, spine bone and rib bone and we normalized the activity concentration in each organ by the total activity uptake, both for real and simulated data. The analysis of the relative differences between quantification values obtained for the real and the simulated data shows differences of 22.7 % for the bladder; 10.3 % for the spine bone and 13.7 % for the rib bone.

B. *Metabolic imaging using FDG*

Results obtained for the FDG radiotracer are presented in Fig. 6.

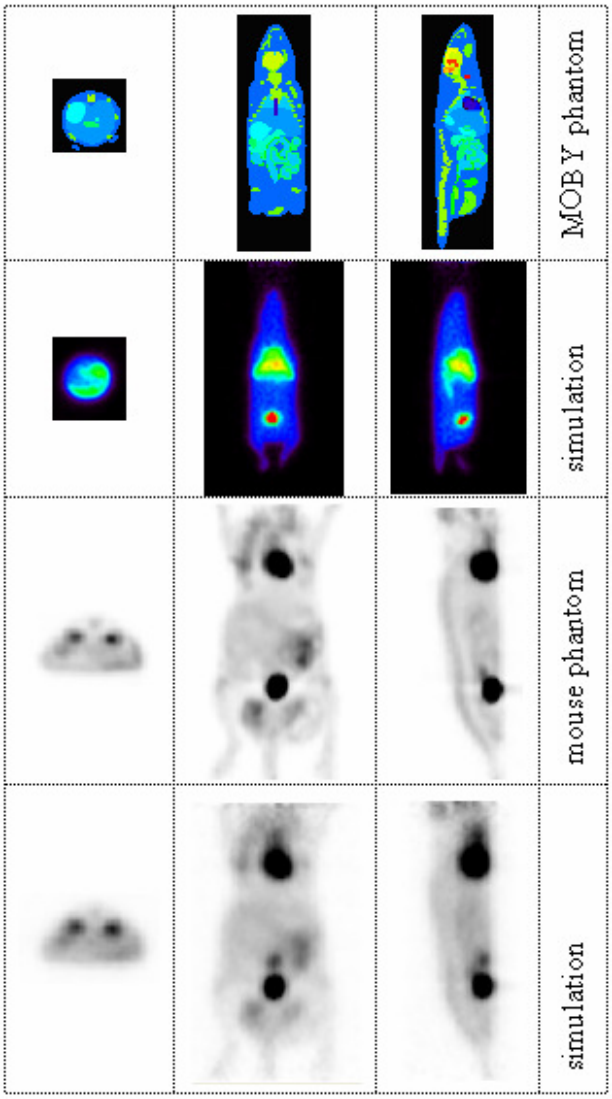

Fig. 6. Images corresponding to the gold standard simulations for the FDG.

Fig. 7 shows the quantitative analysis for the simulated FDG exam with the mouse phantom generated from the real acquisition. We defined ROIs on the liver, bladder, heart and kidneys. The activity concentration in each ROI was normalized by the total activity inside the whole body, both for real and simulated data. The relative differences, between the quantification values

obtained for the simulated data and the real exam, showed differences of 1.8 % for the liver and the heart; 3.7 % for the bladder and 7.5 % for the kidneys. These differences may partly result from small differences on the ROIs definitions in the real exam and simulation.

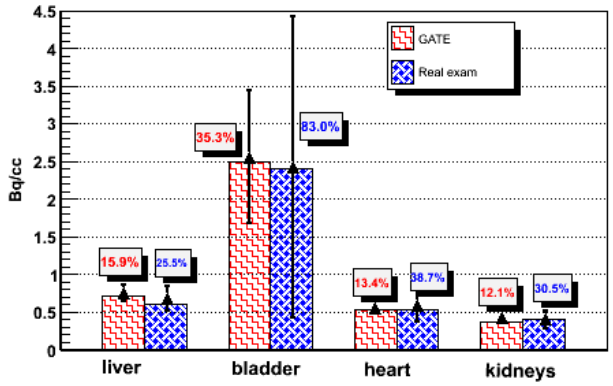

Fig. 7. Comparison between PET image quantification and the GATE measurements. Black bars represented the ROI statistical error measured as the ratio standard deviation over mean for all pixels considered.

Fig. 5 and Fig. 7 also show the statistical error related to each ROI (shown as error bars). These values show that the variability from simulated results is lower than the measurements obtained from the real exams. This difference most probably results from sub-optimal conditions (related with the physical effects) in the real exams.

The TACs related with the gold standard results for the full simulation of an FDG exam, with the MOBY phantom, are presented in Fig. 8. If we compare the simulation against the experimental measurements (Fig. 3), used as input on the simulation, we find some differences in the TACs. These differences can be partially explained by the variability induced by ROIs description, and due to the differences between the anatomical structures of the MOBY phantom against a real mouse.

We have generated an emission dataset using typical values of FDG uptake for each organ at the last acquisition time frame, for the non normal tidal breathing with the MOBY phantom. The result is illustrated in Fig. 9.

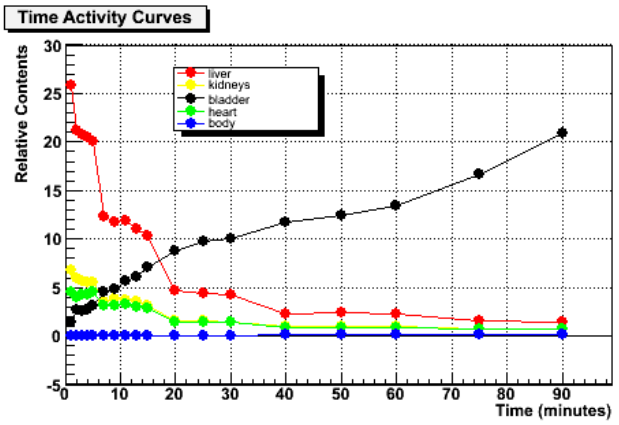

Fig. 8. TACs resulting from the complete FDG simulated exam with the MOBY phantom.

The Fig. 10 shows the result of the simulation of the last frame for an FDG exam including a lung tumor implementation.

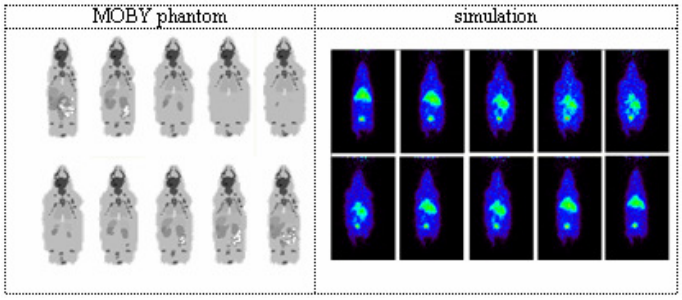

Fig. 9. Coronal slices corresponding to the simulation of the breathing motion, over one respiratory cycle for a FDG exam at the last time frame.

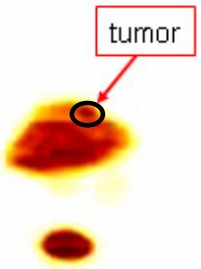

Fig. 10. Maximum Intensity Projection (MIP), resulting from the simulation of the last frame of an FDG exam with a specific tumoral uptake in the lung of the MOBY phantom.

IV. CONCLUSIONS & PERSPECTIVES

The good agreement between simulation and real data leads us to conclude that the GATE platform is a relevant tool to perform small animal PET imaging simulation, under realistic conditions.

This work is now being complemented by accessing the impact of the respiratory motion in the detection of lung lesions. In this context, the optimization of acquisition protocols, image correction procedures and image reconstruction methods will be pursued.

References

[1] Jan, S. et al., "GATE: a simulation toolkit for PET and SPECT," *Physics in Medicine and Biology*, vol. 49, no.19. pp. 4543-4561, August 2004.

[2] Tai, Y. et al., "Performance Evaluation of the microPET FOCUS: A Third-Generation microPET Scanner Dedicated to Animal Imaging," *Journal of Nuclear Medicine*, vol. 46, pp. 455-463, March 2005.

[3] Jan, S. et al., "Monte Carlo simulation of the microPET FOCUS system for small rodents imaging applications," *IEEE Nuclear Science Symposium Conference Record*, vol. 3, pp.1653-1657, October 2005.

[4] William P. Segars, Benjamin M. W. Tsui, Eric C. Frey, G. Allan Johnson, Stuart S. Berr, "Development of a 4-D Digital Mouse Phantom for Molecular Imaging Research," *Molecular Imaging and Biology*, vol. 6, no. 3, pp. 149-159, May-June 2004.